

Proliferative Activity in Human Brain Tumors: Comparison of Histopathology and L-[1-¹¹C]Tyrosine PET

Heleen de Wolde, Jan Pruijm, Mirjam F. Mastik, Jan Koudstaal and Willemina M. Molenaar
Department of Pathology and PET Center, University and University Hospital of Groningen, Groningen,
The Netherlands

To validate the protein synthesis rate (PSR) measured in human brain tumors using L-[1-¹¹C]tyrosine (TYR) PET, the PSR was compared to histopathological parameters that reflect proliferation and protein synthesis. **Methods:** We studied 20 patients who had a brain biopsy and who also underwent a PET study with TYR. Paraffin sections were stained with the monoclonal antibody MIB 1, targeted against the core antigen Ki-67, and nucleolar organizer regions (NORs) were measured as argyrophilic NORs (AgNORs). The TYR uptake was measured by PET, and with a kinetic model, the PSR was determined. **Results:** PSR (nmol/ml/min) ranged from 0.44 to 1.99 (mean, 0.97), Ki-67 labeling indices (%) ranged from 0.9 to 33.5 (mean, 9.5) and AgNOR area (mm²/cm²) ranged from 0.13 to 0.85. No relationship was found between PSR and Ki-67 labeling index or AgNOR area. **Conclusion:** It seems that the PSR and proliferation, as measured by Ki-67, are independent processes. The role of the PSR is uncertain, but it is likely that it can be seen as a marker for the homeostasis of the cell.

Key Words: brain tumors; proliferation; L-[1-¹¹C]TYR; PET; protein synthesis rate

J Nucl Med 1997; 38:1369-1374

The growth rate of brain tumors is an essential feature in establishing their malignancy. To assess tumor proliferation, histopathology is used as the golden standard, although it is known to be fraught with difficulties because of the problems inherent in counting mitoses. In addition, due to the regional heterogeneity of brain tumors, sampling errors may occur. Therefore, other methods for evaluating the proliferative potential are investigated.

In vivo assessment of tumor metabolism can be done by PET (1-3). Radiopharmaceuticals labeled with positron-emitting radioisotopes allow for the quantification of the glucose consumption or the protein synthesis of a tumor, for example (4-7). Several labeled amino acids have been studied to evaluate gliomas (7-10). In our center, the radiopharmaceutical L-[1-¹¹C]tyrosine (TYR) was developed (11), and it has been shown that, with a suitable kinetic model, the protein synthesis rate (PSR) in tumor tissue can be assessed (12,13). Although it has been well established that the incorporation of TYR is a measure of protein synthesis, the biological significance of this finding is as yet undetermined. In a previous study in brain tumors, we were unable to establish a relation between the PSR and the grade of malignancy (14).

In vitro assessment of proliferative activity of tumors has advanced with the development of histopathological techniques, labeling cells in different states of biological activity. Ki-67 (or MIB 1), is a monoclonal antibody that reacts with a

nuclear antigen expressed in the late G₁, S, G₂ and M phases of the cell cycle but not in the G₀. It thus detects nonresting cells and can be considered as a proliferation marker (15-20). Nucleolar organizer regions (NORs) are sites of genes transcribing to ribosomal RNA. They are assumed to be involved in protein synthesis, cell growth and cell differentiation. These NORs can be visualized by the application of a silver-staining method and are then designated argyrophilic NORs (AgNORs) (21,22).

In the current study, we compared the results obtained with TYR PET with histopathological markers, i.e., MIB-1 and AgNOR, in an attempt to validate the PET signal and to obtain a better insight in the proliferative and metabolic capacity of brain tumors.

MATERIALS AND METHODS

Patients and Tissues

Twenty patients, suspected clinically and by imaging of having a primary or metastatic brain tumor, underwent a PET study with TYR at the Groningen University Hospital PET Center. Patient data are listed in Table 1. Patients generally suffered from large tumors: median (PET-assessed) volume was approximately 43 ml (range, 7-207 ml). Three patients had a small tumor (volume, <15 ml): one patient with an oligodendroglioma, one with an anaplastic astrocytoma and one with a cerebral metastasis. A stereotactic biopsy of the tumor was taken in 9 cases, whereas the tumor was removed in 11 cases. In 10 cases, the biopsy was taken before the PET scan was performed (interval time ranged from 3 to 978 days; median, 115 days). Two patients with a glioblastoma had very long periods between the surgical removal of the tumor and their PET scan (978 and 632 days, respectively). The PET was performed because of the suspicion of recurrence, despite treatment with surgery, external radiotherapy and brachytherapy. In the other 10 cases, the PET scan was performed first (interval time ranged from 1 to 55 days; median, 5 days).

Surgical specimens were routinely fixed and embedded in paraffin. Sections of 3 μm were cut, floated in a bath of distilled water and mounted on 3-amino-propyl-ethoxy-silane-coated slides. They were dried overnight at 37°C. Before use, slides were heated for 20 min at 60°C on a hot plate.

PET

In all patients, a dynamic PET study was performed. Patients refrained from food for at least 6 hr before the study but had free access to water and took their normal medication. A venous cannula was placed in the antecubital vein of one of the forearms to allow for easy injection of TYR, and an arterial cannula was placed in the radial artery of the contralateral arm to assess the arterial input function and metabolites. The patient's head was positioned in the whole-body PET camera, parallel to the orbital meatal line. The average spatial resolution amounted to 5.0, 5.1 and 4.8 mm FWHM in the x, y and z direction, respectively, in the

Received Sep. 27, 1996; revision accepted Feb. 3, 1997.

For correspondence or reprints contact: Willemina M. Molenaar, MD, PhD, Department of Pathology, University of Groningen, P.O. Box 30.001, 9700 RB, Groningen, The Netherlands.

TABLE 1
Histopathological Diagnosis, Age and Sex of the Patients, and PSR, Ki-67 LI and AgNOR

Patient no.	Age (yr)	Sex	Histology	Operation	PSR (nmol/ml/min)	Ki-67 LI (%)	AgNOR (mm ² /cm ²)
1	26	F	Meningioma	T	0.93	3.1	0.65
2	21	M	Oligodendroglioma	T	1.83	3.6	0.19
3	38	F	Oligodendroglioma	S	0.89	4.0	0.26
4	27	F	Mixed oligo/astrocytoma	T	0.44	4.5	0.18
5	54	M	Mixed oligo/astrocytoma	S	0.95	0.9	0.36
6	33	M	Astrocytoma	T	0.82	8.4	0.62
7	29	M	Astrocytoma	T	1.13	2.8	0.47
8	44	M	Astrocytoma	S	0.80	1.6	0.27
9	28	F	Astrocytoma	T	0.59	7.7	0.17
10	39	M	Anaplastic astrocytoma	S	0.75	8.2	0.44
11	29	F	Anaplastic astrocytoma	T	1.23	24.9	0.26
12	17	M	Anaplastic astrocytoma	T	0.55	6.9	0.73
13	42	F	Glioblastoma	T	1.99	33.5	0.84
14	59	F	Glioblastoma	T	0.65	7.3	0.13
15	38	F	Glioblastoma	S	0.99	3.8	0.22
16	62	F	Glioblastoma	T	1.10	1.6	0.18
17	69	M	Glioblastoma	S	0.73	16.6	0.85
18	20	M	Glioblastoma	S	0.97	19.3	0.13
19	32	M	Glioblastoma	S	1.47	3.1	0.31
20	55	M	Metastatic carcinoma	S	0.61	27.2	0.33

F = female; M = male; T = total removal; S = stereotaxic biopsy.

center of the field of view. The sensitivity as measured with a 20-cm-diameter, 20-cm-long phantom was 125,000 Hz/37 kBq·ml. After a 20-min transmission scan to correct for attenuation, 370 MBq of TYR was injected through the venous access as a 1-min bolus. Camera acquisition started at the time of injection (time frames 10 × 30, 3 × 300 and 3 × 600 sec). During the study, arterial blood samples were taken for the assessment of the plasma TYR activity curve and of its metabolites (¹¹CO₂ and ¹¹C-labeled proteins). Acid-soluble metabolites (p-hydroxy-phenylpyruvic acid and p-hydroxy-phenyllactic acid) were neglected in the calculation of the PSR because of their late appearance and low concentrations in plasma (13). PET images were displayed in coronal, sagittal and transaxial projections on a computer display applying standard software. For PSR calculations, the tumor was outlined with the aid of dedicated software developed at the PET Center Groningen as described previously (13,14). Tumor definition was done by visual inspection. The activity in the selected pixels was averaged, and the corresponding time-activity curve was calculated. Combining this averaged time-activity data with the plasma input data (corrected for ¹¹CO₂ and ¹¹C-labeled proteins), the average amino acid incorporation, PSR, is calculated in nmol/100 g of tumor tissue/min as described previously (10).

Ki-67 Antigen Labeling

For Ki-67 labeling, the monoclonal antibody MIB 1 was used, which recognizes an epitope of the Ki-67 antigen. Immunohistochemistry was performed on paraffin sections according to a method modified from Shi et al. (23,24). In short, after heating on a hot plate, slides were dewaxed in xylene and rehydrated in serial ethanol washes (100%, 96% and 70%). After being heated twice in an autoclave for 10 min at 110°C in 20 mM citrate buffer (pH 6.0), slides were incubated with a 1:400 dilution of the antibody in maleate buffer (pH 7.4). The primary antibody was detected with a biotinylated secondary antibody (multilink) followed by a streptavidin-alkaline phosphatase conjugate. Final color was developed by the bromochloroindolyl-phosphate 4-nitroblue-tetrazoliumchloride method. Sections were counterstained with hematoxylin and coverslipped with a mounting medium that is soluble in xylene.

AgNOR

Staining was performed according to a modified protocol of the original procedure of Howell and Black (25,26). Sections were dewaxed in xylene, rehydrated in alcohol to water and incubated with freshly prepared AgNOR solution (one volume of 2% gelatin in 1% formic acid mixed with two volumes of 20% aqueous silver nitrate) at 37°C for 30 min. Sections were washed in distilled water, in 1% sodiumthiosulfate for 1 min and again in distilled water. The sections were dehydrated, rinsed in xylene and mounted with a mounting medium.

Quantification

For measuring the Ki-67 labeling index (LI), we used ocular micrometry on a microscope by using an eyepiece grid at ×40 magnification. In histologically viable areas, 30 fields were randomly selected. The positive and negative nuclei were counted. Endothelial cells, inflammatory cells and necrosis were excluded. The Ki-67 LI was defined as the total number of positive nuclei divided by the total number of nuclei. Number and area of AgNORs were quantitatively assessed using an interactive image analysis system consisting of a microscope equipped with a charged coupled device video camera and ×40 objective. A total magnification of ×4840 was realized. The camera was connected to the video input of an image memory board installed on a personal computer. After digitization, a threshold was interactively set so as to measure only AgNORs. The relative area occupied by AgNOR dots compared to surrounding tissue was measured (mm²/cm²). For each tumor, at least 20 randomly selected fields were quantitated.

Statistics

Pearson's product-moment correlation was calculated between the PSR on one hand and Ki-67 LI and AgNOR area on the other. The null hypothesis was that no correlation existed between entities, and this hypothesis would be rejected at a level of p < 0.05. Also, the different entities were compared with histological grade as defined by standard light microscopy. Significance was calculated with the Kruskal-Wallis nonparametric ANOVA and defined at a level of p < 0.05.

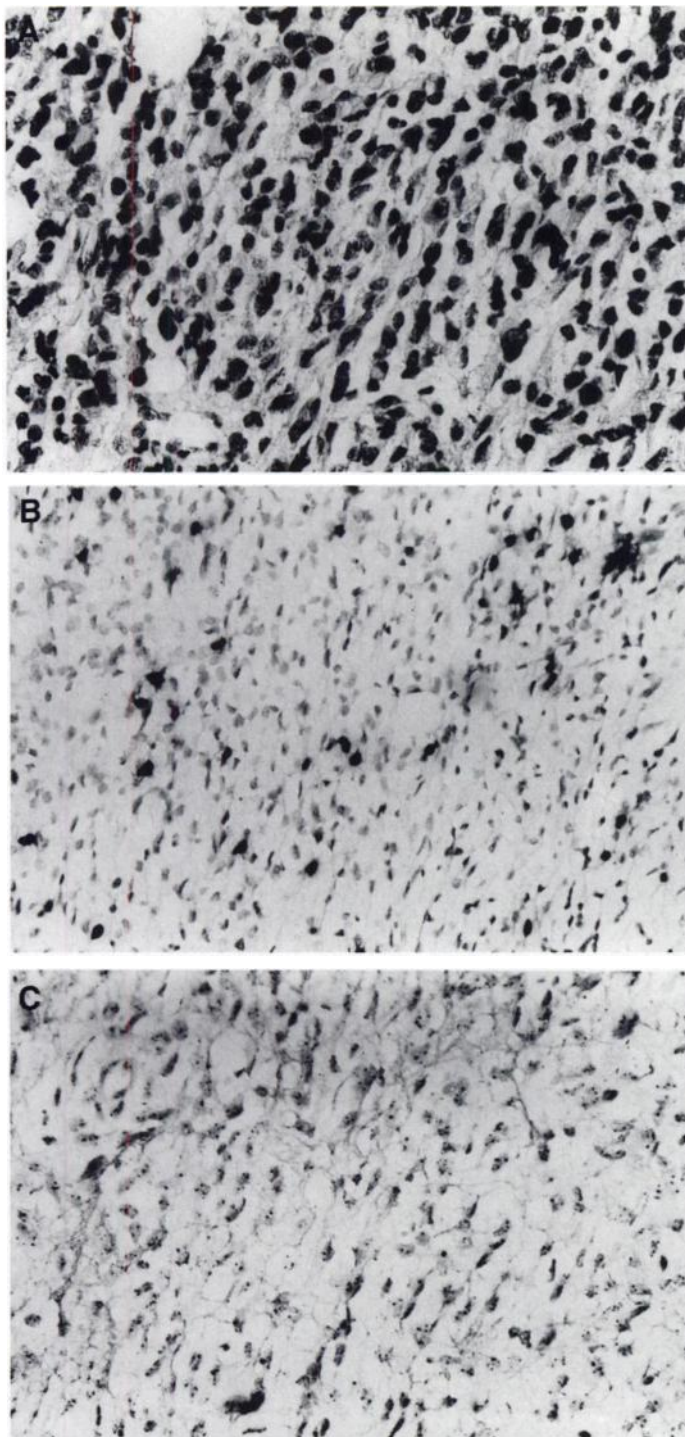


FIGURE 1. Anaplastic astrocytoma (Patient 10). All figures show serial sections obtained from the same patient. (A) Hematoxylin and eosin staining ($\times 400$); (B) MIB 1-positive cells (LI = 8.2%; $\times 256$); (C) AgNORs (AgNOR area = 0.44 mm²/cm²; $\times 550$).

RESULTS

Histological Classification

The tumors were classified on hematoxylin- and eosin-stained paraffin sections (Table 1), applying WHO criteria to primary brain tumors (27,28). Accordingly, 1 meningioma, 2 oligodendrogliomas, 2 mixed oligo-astrocytomas, 4 astrocytomas, 3 anaplastic astrocytomas and 7 glioblastomas were identified. One patient appeared to have a metastatic carcinoma. Figure 1A shows a hematoxylin- and eosin-stained example of Patient 10 in whom an anaplastic astrocytoma was diagnosed.

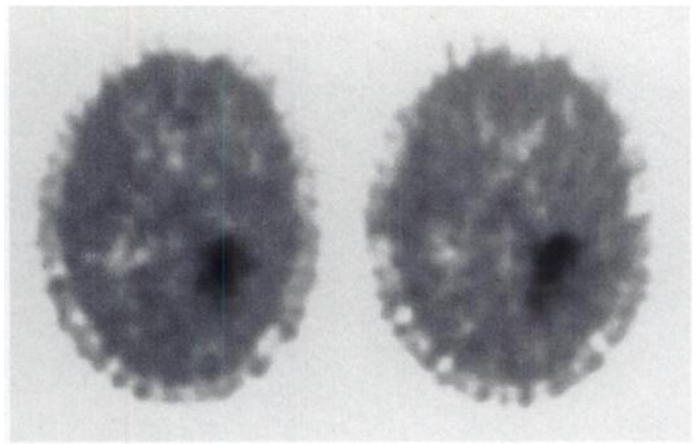


FIGURE 2. PET scan with TYR in Patient 10. The tumor is visible in the left parietal hemisphere. Calculated PSR = 0.75 nmol/ml/min.

PSR

All tumors showed an increased uptake of TYR as compared to background tissue, visible as a "hot spot" on the PET images (Fig. 2). In three glioblastomas (nos. 13, 14 and 18), a "cold spot" was manifest in the center of the hot spot, due to the presence of necrotic tissue. The PSR ranged from 0.44 for a mixed oligo/astrocytoma (no. 4) to 1.99 for a glioblastoma (no. 13) (Table 1).

Ki-67 Immunoreactivity

Darkly stained positive nuclei were clearly distinguishable from negative nuclei (Fig. 1B). They were not homogeneously distributed throughout the tumor but were numerous in some areas and rare or absent in others. Ki-67 LI varied widely between tumors and among different areas in one tumor. Values ranged from 0.9 for a mixed oligo/astrocytoma (no. 5) to 33.5 for a glioblastoma (no. 13) (Table 1).

AgNOR Area

NORs were visible as black, silver-stained dots within the cell nuclei (Fig. 1C). AgNOR areas ranged from 0.13 for two glioblastomas (nos. 18 and 14) to 0.85, also for a glioblastoma (no. 17) (Table 1).

Relationships between PSR, Ki-67 LI, AgNOR Area and Histology

We were unable to demonstrate a relationship between the PSR on one hand and the histopathological diagnosis on the other hand (Fig. 3). The Kruskal-Wallis ANOVA gave an overall significance of 0.56. Also, no significant correlations were present between the Ki-67 LI or AgNOR area with the measured PSR (Fig. 4). No correlation was found between the histological diagnosis and Ki-67 LI or AgNOR count or between Ki-67 LI and AgNOR count.

DISCUSSION

The current study was set up to explore the relationship between the PSR and the proliferative activity of brain tumors using advanced histological techniques that aim at measuring proliferation rate and protein synthesis. Because PET studies are still restricted to a research setting, the number of patients studied with TYR-PET who also underwent brain surgery is necessarily limited. This explains the small and heterogeneous group of patients included. This may also explain the lack of a correlation between histological diagnosis and Ki-67 LI. Previous studies in nonbrain normal and tumor tissues and cell lines have shown a correlation between AgNOR size and mean area and proliferative activity (29-31). In brain tumors, a correlation between AgNOR number, in contrast to the mean area mea-

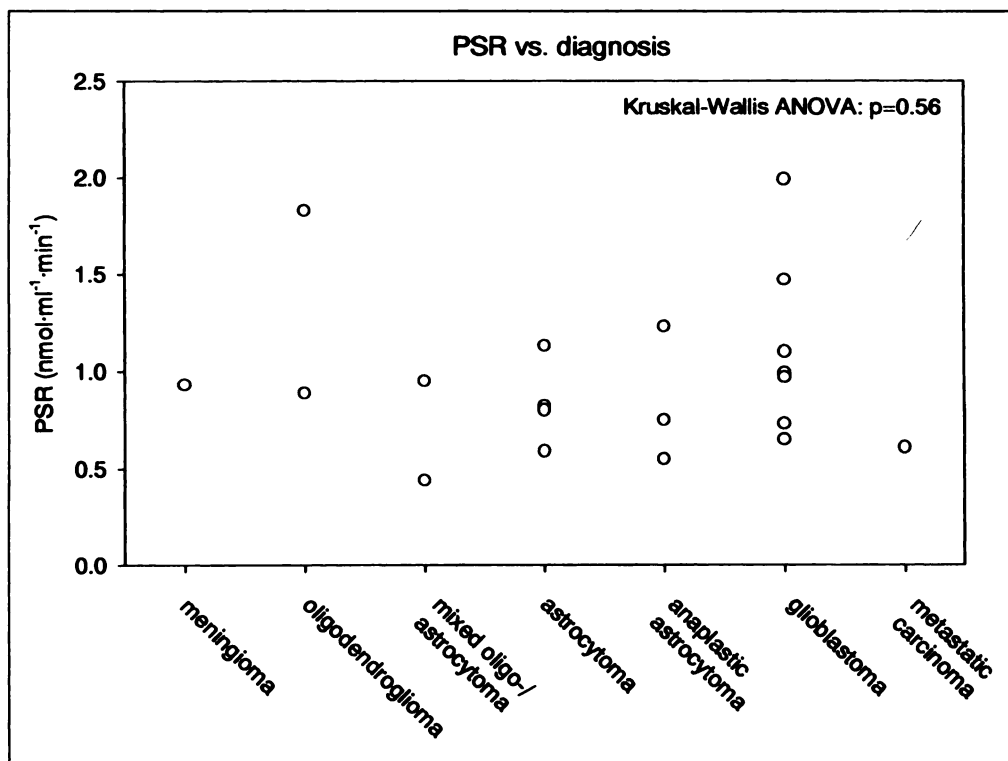


FIGURE 3. Scatter diagram showing the lack of relationship between PSR and histological malignancy grade.

sured in the current study, and proliferation (32) and histological grade (33,34) was established. However, there was much overlap between the different tumor groups, and the significance of AgNORs in the grading of brain tumors is still debatable (33).

Although TYR-PET gave a clear signal in all patients, unfortunately, no correlation between PSR and any of the histological parameters was found. Earlier studies, primarily using the tracers 2-[¹⁸F]fluoro-2-deoxyglucose (FDG) or L-[methyl-¹¹C]methionine (MET), have proven that PET is successful in detecting brain tumors (4-6,35), and a relationship with malignancy grade has been indicated (36,37). The disadvantage of the use of FDG in the brain is the high uptake in normal brain tissue, hampering the differential diagnosis of low-grade tumors because they show up as a cold spot on the image. This drawback can be overcome by using ¹¹C-labeled amino acids. Of these, methyl-labeled MET is most widely used, but in our center, we developed L[¹¹C]TYR for this

purpose instead (11). TYR, in contrast to other amino acids, has a small free TYR pool in plasma and tissue and a high turnover, which makes it an attractive tracer to measure the PSR (10,12,13). Although the validity of the radiopharmaceutical for use in diagnosing brain tumors has been shown, no relationship between the PSR and malignancy grade, as established with standard histological methods, could be assessed so far (14). Several explanations should be considered for this lack of a relation between our in vivo PET data and the in vitro data.

Partial Volume Effect

The quantification of metabolic processes with PET is a complicated technique that may easily go wrong. Several flaws need to be considered, of which the partial volume effect is one of the most important because it may underestimate the activity of the metabolic process quite severely. For instance, a spheroidal tumor with a PET-selected diameter of 5 cm will have a volume of 65.4 ml. However, because of the resolution of the camera of

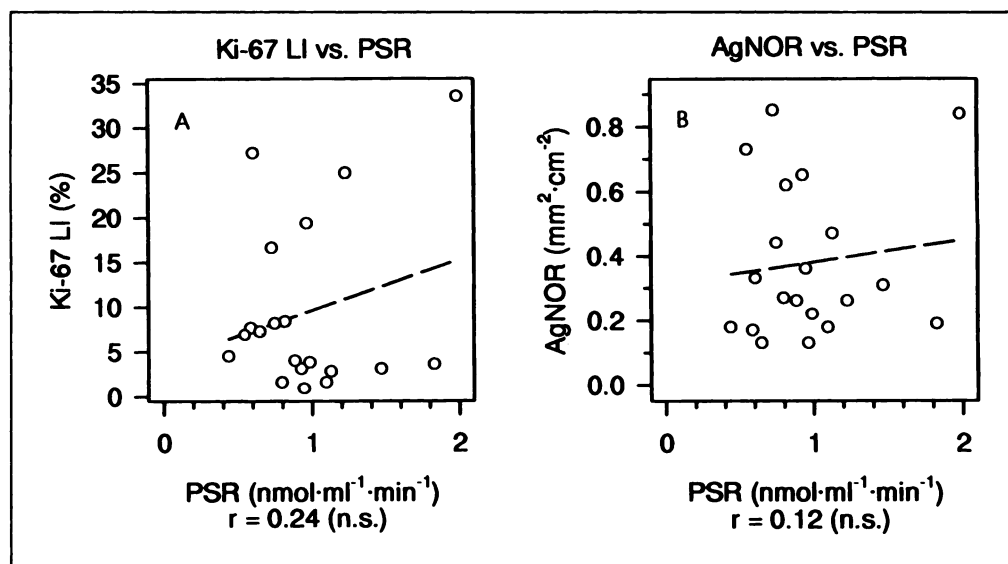


FIGURE 4. Scatter plots showing the relationship between (A) the PSR and Ki-67 LI and (B) PSR and AgNOR area. No significant correlations were present.

5 mm FWHM, the real diameter of the tumor will be $5 - 0.5 = 4.5$ cm, resulting in a volume of 47.7 ml. Thus, the tumor volume is overestimated by:

$$\frac{65.4 - 47.7}{47.7} = \frac{17.7}{47.7} = 37\%$$

and likewise, the PSR is underestimated with this percentage. However, we feel that the effects in this particular study are limited because sizes of the tumors throughout the different histological classes were in the same order of magnitude; thus, the partial volume effects were equally distributed.

Cell Proliferation

Mitotic activity is an important determinant of malignancy grade in brain tumors. Thus, a higher Ki-67 LI is considered to be associated with a high proliferative activity. The lack of correlation between PSR and proliferation as measured by Ki-67 labeling, though disappointing, is in line with our earlier study (14). The findings contrast with those of Sato et al. (37), who, using methyl-labeled MET, found significant differences in uptake of this tracer according to pathological grading, although considerable overlap existed in their series. The discrepancy between TYR and MET should possibly be attributed to the different labeling position of the ^{14}C label. The disadvantage of MET in assessing PSR is that its methyl group is transferred to several methyl acceptors, including DNA (38). In contrast, in carboxyl-labeled amino acids, the label is mainly incorporated into the proteins or washed out by side reactions (decarboxylation and oxidation), which supposedly makes them more suitable for measuring PSR (39). Because it cannot be excluded that the findings with MET as presented in the literature are due to methyl transfer, the lack of a correlation with proliferation in our study may again emphasize the importance of the position of the label within the molecule in PET studies to avoid contamination of the signal with metabolite data. Finally, it may be argued that tumor cell density has more impact on the value of the PSR than on the Ki-67 LI. However, taking cell density into account, no correlation was found either. So far, we have been unable to associate the PSR, as assessed with TYR-PET, with cell proliferation.

AgNOR

AgNORs are involved in protein synthesis. Although in animal studies the PSR was proven to be a measurement of protein synthesis (12), we nevertheless were unable to find a relationship between the in vivo PSR and in vitro AgNOR area. At this stage, an explanation can only be speculative. The first explanation to be considered is the different order of magnitude of assessment, i.e., histopathological markers examine a small tumor sample at a cellular level, whereas the PSR examines the mean of the whole tumor. Sampling error would then be the cause of a discrepancy between the two modalities. However, no differences were apparent between stereotactic tumor biopsies and specimens from totally removed tumors; the latter comprised mostly fragmented specimens obtained by suction, such that each individual histological slide was representative for the whole tumor. There is still uncertainty about the nature of the AgNOR signal. In particular, it is unclear whether there exists a linear relationship between AgNOR surface area and protein synthesis level (40). Also, although the incorporation of TYR is designated as PSR, it would be better to speak of the amino acid incorporation rate. This does not necessarily mean only protein synthesis; it may also include trapping in other biochemical processes. The PET signal cannot differentiate between these different biochemical forms. It could also be that

TYR is involved in tumor cell metabolism in another way, such as cell homeostasis. For this explanation to be valid, it would mean that the assumption that the findings in animal tumors, i.e., over 80% incorporation in proteins, can be extrapolated to the clinical situation needs to be further validated (41).

A likely explanation may also be that, in brain tumors, proliferation and protein synthesis are independent processes, as previously suggested by Onda et al. (42). The PSR could represent a marker for the homeostasis of the cell, including repair mechanisms in which proteins play an essential role, but it is not for proliferation. This would be in line with the observations in atrophic and regenerating rat calf muscles, in which AgNOR counts seemed to parallel protein synthesis not accompanied by proliferation (43), and with the findings in rat experimental pancreatitis, in which AgNORs seemed to be a marker of regulatory cellular processes independent of the total intracellular PSR (44). In a rat model with inoculated C6 glioma cells, Takeda et al. (45) showed the discrepancy in the reaction to chemotherapy of cell proliferation (declined) compared to protein synthesis (remained constant). Their findings also indicate that protein synthesis is not merely a reflection of cell proliferation. To substantiate this hypothesis, an identification of the different cellular proteins into which TYR is built, e.g., through [^{14}C]TYR, is needed.

CONCLUSION

It seems that PSR on the one hand and proliferation as measured by Ki-67 and protein synthesis as assessed by AgNOR counts, on the other are independent processes. An explanation may be that the PSR is involved in the homeostasis of the cell. Despite this lack of relationships between in vitro techniques and in vivo PET, for practical purposes, TYR-PET remains useful for the detection and delineation of brain tumors and their recurrences. The follow-up of patients studied with PET is still too brief to evaluate whether the PSR might be an indicator of prognosis in brain tumors.

ACKNOWLEDGMENTS

This study was supported by a grant of the J. K. de Cock Foundation. We thank T. Wiegman for his technical assistance, S. Noorman for the photographs and Dr. M. Kros for providing biopsies from the Erasmus University Hospital, Rotterdam, The Netherlands.

REFERENCES

1. Coleman RE, Hoffman JM, Hanson MW, Sostman HD, Schold SC. Clinical application of PET for the evaluation of brain tumors. *J Nucl Med* 1991;32:616-622.
2. Byrne TN. Imaging of gliomas. *Semin Oncol* 1994;21:162-171.
3. Olivero WC, Dulebohn SC, Lister JR. The use of PET in evaluating patients with primary brain tumors: is it useful? *J Neurol Neurosurg Psychiatr* 1995;57:250-252.
4. Di Chiro G, Brooks RA, Patronas NJ, et al. Issues in the in vivo measurement of glucose metabolism of human central nervous system tumors. *Ann Neurol* 1984; 15(suppl):S138-S146.
5. Glantz MJ, Hoffman JM, Coleman RE, et al. Identification of early recurrence of primary central nervous system tumors by [^{18}F]fluorodeoxyglucose positron emission tomography. *Ann Neurol* 1991;29:347-355.
6. Di Chiro G. Positron emission tomography using [^{18}F]fluorodeoxyglucose in brain tumors: a powerful diagnostic and prognostic tool. *Invest Radiol* 1986;22:360-371.
7. Vaalburg W, Coenen HH, Crouzel C, et al. Amino acids for the measurement of protein synthesis in vivo by PET. *Nucl Med Biol* 1992;19:227-237.
8. Derlon JM, Bourdet C, Bustany P, et al. Carbon-11-L-methionine uptake in gliomas. *Neurosurgery* 1989;25:720-728.
9. Vaalburg W, Elsinga PH, Paans AMJ. Carbon-11 amino acids, labeling and metabolites. In: *PET studies on amino acid metabolism and protein synthesis*. Dordrecht: Kluwer Academic; 1993:75-80.
10. Paans AMJ, Vaalburg W, Woldring MG. A comparison of the sensitivity of PET and NMR for in vivo quantitative metabolic imaging. *Eur J Nucl Med* 1985;11:73-75.
11. Bolster JM, Vaalburg W, Paans AMJ, et al. Carbon-11-labeled tyrosine to study tumor metabolism by PET. *Eur J Nucl Med* 1986;12:321-324.
12. Ishiwata K, Vaalburg W, Elsinga PH, Paans AMJ, Woldring MG. Metabolic studies with L[1- ^{14}C]tyrosine for the investigation of a kinetic model to measure protein synthesis rates with PET. *J Nucl Med* 1988;29:524-529.

13. Willemsen ATM, van Waarde A, Paans AMJ, et al. In vivo protein synthesis rate determination in primary or recurrent brain tumors using L-[1-¹¹C]-tyrosine and PET. *J Nucl Med* 1995;36:411-419.
14. Pruijm J, Willemsen A, Molenaar WM, et al. Brain tumors: L[1-¹¹C]tyrosine PET for visualization and quantification of protein synthesis rate. *Neuroradiology* 1995;197:221-226.
15. Gerdes J, Lemke H, Baisch H, Wacker HH, Schwab U, Stein H. Cell cycle analysis of a cell proliferation-associated human nuclear antigen defined by the monoclonal antibody Ki-67. *J Immunol* 1984;133:1710-1715.
16. Zuber P, Hamou MF, de Tribolet N. Identification of proliferating cells in human gliomas using the monoclonal antibody Ki-67. *Neurosurgery* 1988;22:364-368.
17. Raghavan R, Steart PV, Weller RO. Cell proliferation patterns in the diagnosis of astrocytomas, anaplastic astrocytomas and glioblastoma multiforme: a Ki-67 study. *Neuropathol Appl Neurobiol* 1990;16:123-133.
18. Giangaspero F, Doglioni C, Rivano MT. Growth fraction in human brain tumors defined by the monoclonal antibody Ki-67. *Acta Neuropathol* 1987;74:179-182.
19. Catoretti G, Becker MHG, Key G, et al. Monoclonal antibodies against recombinant parts of the Ki-67 antigen (MIB 1 and MIB 3) detect proliferating cells in microwave-processed formalin-fixed paraffin sections. *J Pathol* 1992;168:357-363.
20. Karamitopoulou E, Perentes E, Diamantis I, Maraziotis T. Ki-67 immunoreactivity in human central nervous system tumors: a study with MIB 1 monoclonal antibody on archival material. *Acta Neuropathol* 1994;87:47-54.
21. Bloom SE, Goodpasture C. An improved technique for selective silver staining of nucleolar organizer regions in human chromosomes. *Hum Genet* 1976;34:199-206.
22. Lindler LE. Improvements in the silver-staining technique for nucleolar organizer regions (AgNOR). *J Histochem Cytochem* 1993;41:439-445.
23. Shi SR, Key ME, Kalra KL. Antigen retrieval in formalin-fixed, paraffin-embedded tissues: an enhancement method for immunohistochemical staining based on microwave oven heating of tissue sections. *J Histochem Cytochem* 1991;39:741-748.
24. Emanuels A, Hollema H, Koudstaal J. Autoclave heating: an alternative method for microwaving? *Eur J Morphol* 1994;32:337-340.
25. Howell WM, Black DA. Controlled silverstaining of nucleolus organizer regions with a protective colloidal developer: a 1-step method. *Experientia* 1980;36:1014-1015.
26. Emmers R. The AgNOR staining: a quantitative and qualitative study [in Dutch]. *Histotechniek* 1990;9:109-115.
27. Kleihues P, Burger PC, Scheithauer BW. The new WHO classification of brain tumors. *Brain Pathol* 1993;3:255-268.
28. Kleihues P, Burger PC, Scheithauer BW. *Histological typing of tumors of the central nervous system*. Berlin; Springer Verlag: 1993.
29. Leek RD, Alison MR, Sarrab CE. Variations in the occurrence of silver-staining nucleolar organizer regions (AgNORs) in non-proliferating and proliferating tissues. *J Pathol* 1991;165:43-51.
30. Trerè D, Farabegoli F, Cancellieri A, Ceccarelli C, Eusebi V, Derenzini M. AgNOR area in interphase nuclei of human tumors correlates with the proliferative activity evaluated by bromodeoxyuridine labeling and Ki-67 immunostaining. *J Pathol* 1991;165:53-59.
31. Derenzini M, Pession A, Trerè D. Quantity of nucleolar silver-stained proteins is related to proliferating activity in cancer cells. *Lab Invest* 1990;63:137-140.
32. Korkolopoulou P, Christodoulou P, Papanikolaou A, Thomas-Tsagli E. Proliferating cell nuclear antigen and nucleolar organizer regions in CNS tumors: correlation with histological type and tumor grade. A comparative study of 82 cases on paraffin sections. *Am J Surg Pathol* 1993;17:912-919.
33. Louis DN, Meehan SM, Ferrante RJ, Hedley-Whyte ET. Use of the silver nucleolar organizer region (AgNOR) technique in the differential diagnosis of central nervous system neoplasia. *J Neuropathol Exp Neurol* 1992;51:150-157.
34. Shirahishi T, Tabuchi K, Mineta T, Momozaki N, Takagi M. Nucleolar organizer regions in various human brain tumors. *J Neurosurg* 1991;74:979-984.
35. Daemen BJG, Zwertbroek R, Elsinga PH, Paans AMJ, Doorenbos H, Vaalburg W. PET studies with L[1-¹¹C]tyrosine, L[methyl-¹¹C]methionine and ¹⁸F in prolactinomas in relation to bromocryptine treatment. *Eur J Nucl Med* 1991;18:453-460.
36. Bustany P, Chatel M, Delron JM, et al. Brain tumor protein synthesis and histological grades: a study by PET with ¹¹C-L-methionine. *J Neurooncol* 1986;3:397-404.
37. Sato K, Kameyama M, Ishiwata K, Hatazawa J, Katekura R, Yoshimoto T. Dynamic study of methionine uptake in glioma using positron emission tomography. *Eur J Nucl Med* 1992;19:426-430.
38. Daemen BJG, Elsinga PH, Ishiwata K, Paans AMJ, Vaalburg W. A comparative study using different ¹¹C-labeled amino acids in Walker 256 carcinosarcoma-bearing rats. *Nucl Med Biol* 1990;18:197-204.
39. Ishiwata K, Kubota K, Murakami M, et al. Re-evaluation of amino acid PET studies: can the protein synthesis rate in brain and tumor tissues be measured in vivo? *J Nucl Med* 1993;34:1936-1943.
40. Delahunt B, Bethwaite PB, Nacey JN, Ribas JL. Proliferating cell nuclear antigen (PCNA) expression as a prognostic indicator for renal cell carcinoma: comparison with tumor grade, mitotic index and silver-staining nucleolar organizer region members. *J Pathol* 1993;170:471-477.
41. Van Langevelde A, van der Molen HD, de Korver-Journee JG, Paans AM, Pauwels EK, Vaalburg W. Potential radiopharmaceuticals for the detection of ocular melanoma. Part III. A study with ¹⁴C and ¹¹C-labeled tyrosine and dihydroxyphenylalanine. *Eur J Nucl Med* 1988;14:382-387.
42. Onda K, Davis RL, Wilson CB, Hoshino T. Regional differences in bromodeoxyuridine uptake, expression of Ki-67 protein and nucleolar organizer region counts in glioblastoma multiforme. *Acta Neuropathol* 1994;87:586-593.
43. Josza L, Kannus P, Jarvinen M, Isola J, Kvist M, Lehto M. Atrophy and regeneration of rat calf muscles cause reversible changes in the number of nucleolar organizer regions. *Lab Invest* 1993;69:231-237.
44. Ruschoff J, Elsassner HP, Adler G. Correlation of nucleolar organizer regions with secretory and regenerative process in experimental cerulein-induced pancreatitis in the rat. *Pancreas* 1995;11:154-159.
45. Takeda N, Diksic M, Yamamoto YL. The sequential changes in DNA synthesis, glucose utilization, protein synthesis and peripheral benzodiazepine receptor density in C6 brain tumors after chemotherapy to predict the response of tumors to chemotherapy. *Cancer* 1996;77:1167-1179.

Prediction of Myelotoxicity Using Radiation Doses to Marrow from Body, Blood and Marrow Sources

Sang-Moo Lim, Gerald L. DeNardo, Diane A. DeNardo, Sui Shen, Aina Yuan, Robert T. O'Donnell and Sally J. DeNardo
University of California Davis Medical Center, Sacramento, California; and Veteran's administration, Northern California Health Care System, California

Bone marrow is generally the dose-limiting organ in radioimmunotherapy (RIT). Although radiation doses to marrow estimated from tracer doses have been shown to be comparable to those from therapy doses of radionuclide, the correlation of marrow radiation dose and myelotoxicity has not been well documented. The purpose of this study was to evaluate the relationship between radiation dose to marrow and subsequent changes in peripheral blood cell counts. **Methods:** Radiation doses to marrow from three sources, body, blood and marrow targeting, were compared with changes in blood counts after the first therapy dose of ¹³¹I-Lym-1 in 16 patients. Doses of ¹³¹I-Lym-1 ranged from 1.1-8.2 GBq (29-222 mCi). Cumulated radioactivity in the body and marrow were obtained using sequential, quantitative images of the body and lumbar vertebrae, respectively, and that in blood using activity in blood samples. The individual and sum of radiation doses from penetrating radiations in the body, and nonpenetrating radiations in the blood and marrow, were compared

with blood counts. **Results:** In this group of patients, median radiation doses were 15.1, 15.4 and 42.1 cGy from body, blood and marrow targeting, respectively. Linear regression of radiation doses from body and blood versus fractional decreases in blood counts produced correlation coefficients of 0.38, 0.06, 0.22 and less than 0.01 for platelets, granulocytes, white blood cells (WBCs) and hematocrit, respectively. Linear regression of targeted marrow radiation doses versus fractional decreases in blood counts produced correlation coefficients 0.61, 0.31, 0.54 and 0.20 for platelets, granulocytes, WBCs and hematocrit. The closest association was found between radiation dose to marrow from marrow targeting and change in platelet count ($r = 0.61$). **Conclusion:** In patients, such as those with non-Hodgkin's lymphoma (NHL), likely to have marrow targeting, prediction of myelotoxicity by conventional body and blood contributions to marrow is substantially improved by the use of radiation dose to marrow estimated from images.

Key Words: dosimetry; myelotoxicity; radioimmunotherapy; iodine-131-Lym-1

J Nucl Med 1997; 38:1374-1378

Received Sep. 23, 1996; revision accepted Jan. 20, 1997.

For correspondence or reprints contact: G.L. DeNardo, MD, Molecular Cancer Institute, School of Medicine, UC Davis, 1508 Alhambra Blvd. #214, Sacramento, CA 95816.